

## Electromagnetic transition between molecular resonances in ${}^8\text{Be}$

D R CHAKRABARTY

Nuclear Physics Division, Bhabha Atomic Research Centre, Mumbai 400 085, India  
E-mail: dr\_chakrabarty@yahoo.com

**DOI:** 10.1007/s12043-014-0858-7; **ePublication:** 4 November 2014

**Abstract.** The nucleus  ${}^8\text{Be}$  has been conjectured to resemble a molecule of two interacting  $\alpha$ -particles. A crucial test of this conjecture is the electromagnetic transition between the molecular resonances. This paper discusses the earlier indirect bremsstrahlung measurements and describes a recent experiment on the direct measurement of  $\gamma$ -transition between the  $4^+$  and  $2^+$  resonances. Experimental results are compared with various theories. The outlook on the measurement of  $2^+ \rightarrow 0^+$  transition will be presented.

**Keywords.** Alpha-cluster model; molecular resonances; gamma transition; *ab-initio* calculation.

**PACS Nos** 21.60.De; 23.20.Js; 25.55.-e; 27.20.+n

### 1. Introduction

One of the many interesting aspects of the atomic nucleus is that under suitable conditions, it deviates from having a homogeneous distribution of neutrons and protons and prefers clustering of a few nucleons. This is the effect of correlations present beyond the mean-field description of the nucleus. The  $\alpha$ -clustering is seen and/or postulated as the most prevalent one because the  $\alpha$ -particle represents the smallest nucleus with a high binding energy per nucleon (7.1 MeV). It is 80% of the highest value (8.8 MeV) seen in  ${}^{62}\text{Ni}$ . Multi- $\alpha$  cluster states, in  $4n$  self-conjugate nuclei, are most probable at excitation energies near the corresponding break-up thresholds. This has been postulated and elucidated in the celebrated Ikeda diagram [1]. One example of this is the famous Hoyle state in  ${}^{12}\text{C}$  [2]. In  ${}^8\text{Be}$ , the ground state should have such a configuration because its energy is slightly above the break-up threshold. A full understanding of the structure of  ${}^8\text{Be}$  is important to understand  $\alpha$ -clustering in heavier nuclei in a better way.

The experimental suggestion for the  $\alpha$ -cluster structure in  ${}^8\text{Be}$  initially came from  $\alpha$ - $\alpha$  scattering experiments [3] done more than 50 years ago. Strong resonances were observed with spin-parity  $0^+$ ,  $2^+$  and  $4^+$ . The corresponding excitation energies (0.0, 3.0 and 11.4 MeV) in  ${}^8\text{Be}$  could be represented as a rotational band of a  $2$ - $\alpha$  molecule. Recent

state-of-the-art *ab-initio* Monte Carlo calculations [4], starting from the basic nucleon–nucleon interaction, also suggest such a molecular representation. The calculated nucleon density distribution clearly shows two separated  $\alpha$ -particles in the ground and excited states, the separation being essentially similar for all the states.

Electromagnetic properties and transitions present a crucial test for any model or theory. This paper is concerned with the electromagnetic transition from the excited states in  ${}^8\text{Be}$ . Two restricted measurements [5,6] on this have been reported about 40 years back. Bremsstrahlung  $\gamma$ -ray emission was measured in  $\alpha$ – $\alpha$  collision experiment without directly detecting the  $\gamma$ -rays. The total kinetic energy of the outgoing  $\alpha$ -particles is less than that in the incoming channel if a bremsstrahlung  $\gamma$ -ray is emitted. In these experiments, the outgoing particles were detected at equal fixed angles and, thus, the intermediate bremsstrahlung  $\gamma$ -ray energy had a definite value for a particular beam energy. The bremsstrahlung cross-section was measured for a range of beam energies. The final excitation energy range in  ${}^8\text{Be}$ , in both the cases, engulfed the  $2^+$  resonance although the initial energies were well below the  $4^+$  resonance.

A series of theoretical calculations was reported to explain these data. The first [5,6] was a model-independent bremsstrahlung calculation considering only the external contribution arising from radiation from the scattering states. The next calculation [7] included the internal contribution corresponding to a transition to the  $2^+$  state in the interior region. The calculations came closer to the data but the comparison was not satisfactory. A microscopic cluster model calculation [8] was done within the framework of the generator coordinate method with fully antisymmetric wave functions in the interior region. Both phase shifts in the elastic scattering and the bremsstrahlung cross-sections were calculated. The authors concluded that a proper reproduction of the phase shifts is necessary for a good reproduction of the bremsstrahlung cross-section.

In order to address this conclusion, the next calculation [9] was done within the  $\alpha$ -cluster model using phenomenological potentials tuned to reproduce the phase shifts. Two philosophically different potentials [10,11], both respecting the Pauli principle in the interior region, could explain the scattering data. In the first, a short-range repulsion was introduced besides the attractive component. In the second (Buck potential), the potential was attractive at all distances. However, the calculated bound states were discarded as the non-allowed ones and the resonance states were orthogonal to the bound states. The nodal structure of the wave functions in the interior region is thus very different in the two cases.

Interestingly, with both the potentials, the bremsstrahlung data could be reasonably well reproduced. This implies that the two restricted measurements reported so far, could not properly probe the internal region and address the structure of  ${}^8\text{Be}$ . An unrestricted measurement of  $\gamma$ -transition between the two resonances should address the relevant issue. This was demonstrated by a calculation [9] of the  $4^+$  to  $2^+$  transition using the two potentials. The results, as expected, differed by a factor of two, the peak cross-sections being  $\sim 260$  and  $130$  nb, respectively. However, no experiment was performed to compare with the calculations. In relatively recent years, the *ab-initio* calculation of the reduced transition probability  $B(E2)$  for the  $4^+$  to  $2^+$   $\gamma$ -transition was done [12]. The preliminary result agreed better with that from the Buck potential.

It is clear that an experimental measurement of  $\gamma$ -transition between the molecular resonances in  ${}^8\text{Be}$ , via a direct detection of the  $\gamma$ -rays, is very important. This should

establish firmly, or seriously question, the  $\alpha$ -cluster structure in  $^8\text{Be}$ . If the findings are in affirmative, a comparison with various theories will provide valuable information on nuclear structure. It may be mentioned here that a direct measurement of  $\gamma$ -transition between resonances has not yet been reported for any system.

## 2. Experimental measurements

The principle of the measurements reported in this paper is to populate  $^8\text{Be}$  across the  $4^+$  resonance and measure the transition  $\gamma$ -ray to the final  $2^+$  state. The two  $\alpha$ -particles following the decay of the final state were detected in coincidence with the  $\gamma$ -rays. Such a triple coincidence measurement is necessary to reduce the background problem which is particularly serious in this case because the expected branching for the  $\gamma$ -decay is  $\sim 10^{-7}$ . In this measurement, a two-dimensional (2D) plot of the  $\gamma$ -ray energy ( $E_\gamma$ ) vs. the total kinetic energy of the two  $\alpha$ -particles should appear as a blob at the appropriate position. The width of the blob is decided by the width of the final state ( $\sim 1.5$  MeV) and the finite detector resolutions.

The experiment was performed at the Pelletron Linac Facility, Mumbai, using  $\alpha$ -beams of 19.2, 22.4, 24.7, 28.9 MeV energy. The target was pure helium gas held in a chamber and isolated from the beam line vacuum by  $1\text{ mg/cm}^2$  kapton foils. Alpha particles were detected in a  $500\text{ }\mu\text{m}$  thick annular Si strip detector [13] with an inner and outer diameter of 4.8 and 9.6 cm, respectively. The double-sided detector, with 32  $\theta$ -rings – in equal left (L) and right (R) halves – on one side and 16  $\phi$ -sectors on the other, was kept at 7 cm from the centre of the chamber in the forward direction. Gamma rays were detected in two 19-BGO (bismuth germanate) arrays placed above and below the central region at about 7 cm. Each BGO was hexagonal in shape with  $\sim 5.7$  cm face-to-face distance and a length of 7.6 cm. The arrays were shielded with heavymets against the 4.44 MeV  $\gamma$ -rays produced in the interaction of the  $\alpha$ -beam with the kapton windows. The scattered  $\alpha$ -particles from the entrance window were stopped before reaching the strip detector by placing a limiting aperture in the central region. Figure 1 shows the schematic of the experimental set-up.

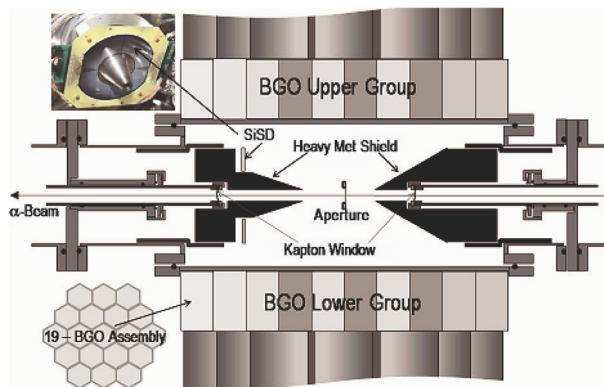


**Figure 1.** Schematic of the experimental set-up.

### 3. Data analysis

Data were collected in an event-by-event mode using a computer-based data acquisition system [14]. The parameters recorded in each event were the energy and the time for the 38 BGO-detector and 48 strip-detector elements. In the data analysis, appropriate conditions were set for the accepted parameters to define a good event. The first condition was the prompt coincidence ( $<10$  ns) between the  $\gamma$ -detector, one of the L-rings and one of the R-rings. The second was the coincidence between the opposite sectors. These conditions emphasized the good events because by neglecting the  $\gamma$ -ray kick, the two  $\alpha$ -particles would move in azimuthally opposite directions. After constructing the total energy ( $E_{\text{sum}}$ ) and total momentum ( $P_{\text{sum}}$ ) of the two detected  $\alpha$ -particles, the other condition was to accept events only within the allowed region of  $E_{\text{sum}}-P_{\text{sum}}$  correlation. This region was guided by a simulation calculation done at all beam energies, which will be discussed later.

Figure 2 shows the 2D spectrum between  $E_{\text{sum}}$  and  $E_{\gamma}$  extracted after the data analysis at one beam energy. The blob shown in the marked region corresponds to the  $\gamma$ -transition between the molecular resonances. The 2D spectrum was converted to a 1D spectrum of total energy  $E_{\text{tot}} = E_{\text{sum}} + E_{\gamma}$  using appropriate ranges of  $E_{\text{sum}}$  and  $E_{\gamma}$ . These ranges were also guided by the simulation calculations. Figure 3 shows the  $E_{\text{tot}}$  spectra at all four beam energies. The peaks seen in the spectra represent the  $\gamma$ -transition to the final state. The peak is absent at the last beam energy which is well off the  $4^+$  resonance.

### 4. Monte Carlo simulation

The extraction of  $\gamma$ -transition cross-sections from the spectra of figure 3 needs a Monte Carlo simulation of the experimental set-up. The simulation was done in two parts, one,

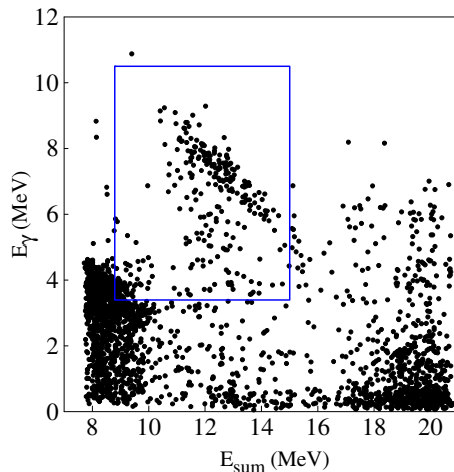


**Figure 2.** Two-dimensional spectrum between  $E_{\text{sum}}$  and  $E_{\gamma}$ , at  $E_{\text{beam}} = 22.4$  MeV. The marked events are selected to create the one-dimensional spectrum in figure 3.

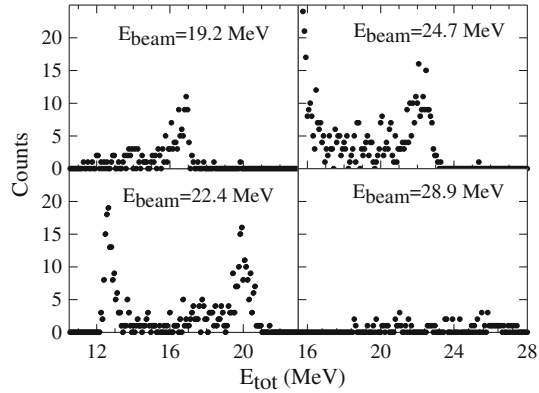


**Figure 3.** One-dimensional spectra of  $E_{\text{tot}} = E_{\text{sum}} + E_{\gamma}$  generated with proper cuts at four beam energies.

for the detection of  $\alpha$ -particles and the other, for the  $\gamma$ -rays, with an aim of getting the spectral shapes and detection efficiencies. The main points considered in the simulation were: (1) the energy loss and angular straggling of the  $\alpha$ -particles in the target gas, (2) angular distributions of the  $\gamma$ -rays and the  $\alpha$ -particles and (3) the  $\gamma$ -ray detector response. The angular distribution of the  $\gamma$ -rays was calculated for the transition from  $J_i = 4$  to  $J_f = 2$  state assuming  $M_i = 0$  and summing over  $M_f$  values weighted by the relevant Clebsch–Gordan coefficients. The angular distribution of the  $\alpha$ -particles was calculated for the decay from these  $(J_f, M_f)$  states, assuming the same weightage values, to the final  $0^+$  state. The  $\gamma$ -ray detector response was calculated with the GEANT3 [15] simulation program after applying the Doppler correction. The outputs of the simulation calculation were the effective target thickness and the absolute detection efficiency for the peak regions shown in figure 3. These quantities along with the beam charge for a given energy were used ultimately to extract the cross-sections. The effective  $\alpha$ -particle energies at the centre of the target were also obtained from the simulation of all beam energies.

## 5. Results and discussion

The extracted  $\gamma$ -transition cross-sections are shown in figure 4. The figure also contains our earlier results [16] at two beam energies. The latter ones have larger error bars because the background problem was not handled as efficiently as in the present work. At this stage, it may be mentioned that in a very recent paper [17], elaborate calculations within the microscopic cluster model have been reported again. The authors focus on the proper handling of the electromagnetic operator. The calculations agree with our earlier data and also reasonably reproduce the old bremsstrahlung data.

A comparison of the experimental peak cross-section with the cluster model calculations [9], using phenomenological potentials, shows that the data favour the Buck potential. A detailed study has been made by comparing with the calculation performed by the authors [18] for three partial waves of angular momentum  $L = 0, 2$  and  $4$ ,

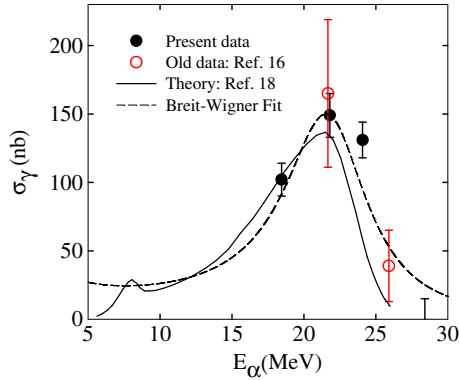


**Figure 4.** Extracted  $\gamma$ -transition cross-sections plotted against the effective  $\alpha$ -particle energy (see text). The last point indicates the upper bound of the cross-section. The continuous line shows the result of the cluster model with Buck potential. The dashed line shows the Briet–Wigner fit to the data.

containing both resonant and non-resonant contributions. This is shown in figure 4, where the contributions from different  $L$  values are summed incoherently. A good agreement is seen in the rising part of the resonance profile but not on the falling side. This could be due to the incoherent summing. On the other hand, this could signify some inadequacy of the phenomenological potential in its detailed aspect like the energy dependence.

We now address the comparison of our data with the results of the *ab-initio* calculations. These calculations were done by the Argonne group using the Argonne  $v_{18}$  two-body and Illinois-7 three-body interactions. The two-body potential reproduced  $np$  and  $pp$  scattering data over a wide energy range of up to 350 MeV. The calculations achieved an excellent reproduction of the spectroscopic properties of  $A \leq 9$  nuclei. Some details of the calculation of the electromagnetic properties of  ${}^8\text{Be}$  are discussed in [19]. The quadrupole moment  $Q = -9.1$  and  $-12.0 \text{ fm}^2$  for the  $2^+$  and  $4^+$  states, respectively, are consistent with a similar intrinsic value of  $Q_0 \sim 32 \text{ fm}^2$ . The  $B(E2)$  values for the  $4^+ \rightarrow 2^+$  transition are presented in table 1.

For the comparison of the result with our data, an effective  $B(E2)$  value has to be estimated. For an approximate estimate, a Briet–Wigner line shape was fitted to the data using the experimental resonance energy and the known width (3.5 MeV) of the  $4^+$  state. From the fit, shown by the dashed curve in figure 4, the  $\gamma$  width and the  $B(E2)$  values were extracted. The  $B(E2)$  value of  $21 \pm 2.3 e^2 \text{ fm}^4$ , is not in very good agreement with the *ab-initio* calculation (table 1). However, it is difficult to draw a quantitative

**Table 1.**  $B(E2)$  values in units of  $e^2 \text{ fm}^4$  from phenomenological cluster model (CM), *ab-initio* calculation (AB) and estimated from experiment (EX).

Transition	CM	AB	EX
$4^+ \rightarrow 2^+$	20.0	$27.2 \pm 0.2$	$21.0 \pm 2.3$
$2^+ \rightarrow 0^+$	57.0	$20.0 \pm 0.8$	–

conclusion because the present estimate is approximate. A better comparison is possible if the *ab-initio* calculation is done for the cross-section as a function of energy. This implies combining the reaction and structure aspects. Such calculation in other system like  $n-\alpha$  scattering has been reported [20].

An interesting aspect is revealed if one considers the theoretical results for the  $2^+$  to  $0^+$  transition in  $^8\text{Be}$ . The cluster-model calculation [18] with the Buck potential shows a much lower peak cross-section compared to the earlier transition (14 nb vs. 134 nb), although this corresponds to a larger  $B(E2)$  value. This is because the transition energy is less by a factor of  $\sim 2.8$ . A comparison of the cluster model results (with Buck potential) and the *ab-initio* calculations (table 1) shows a very large difference. The point to consider is that the  $B(E2)$  values from the *ab-initio* calculations for the two transitions scale as that expected from the Clebsch–Gordan coefficients. This, again, signifies a similar intrinsic deformation for all the states. This is not the case with the cluster model and effectively suggests that the deformation in  $^8\text{Be}$  changes with spin. This fundamental issue can be addressed by measuring the  $2^+$  to  $0^+$   $\gamma$ -transition.

## 6. Summary and outlook

In summary, the  $\gamma$ -transition between the excited states in  $^8\text{Be}$  has been discussed. An experiment measuring the transition between the  $4^+$  and  $2^+$  resonances has been described. The experimental results firmly establish the  $\alpha$ -cluster configuration of  $^8\text{Be}$  by identifying the resonances as molecular states. A comparison with theoretical calculations has been done bringing out the need for a more elaborate *ab-initio* calculation that combines structure with an appropriate reaction model.

In future, the more challenging measurement of the  $\gamma$ -transition between the  $2^+$  and  $0^+$  resonances in  $^8\text{Be}$  should be made. This, however, is expected to have a lesser cross-section and a  $\gamma$ -decay branch of  $\sim 5 \times 10^{-9}$ . Moreover, in the present method, the lower energy  $\alpha$ -particles would be stopped in the gas unless the pressure is kept very low. This, in turn, would correspond to a much smaller target thickness and an unthinkable beam time requirement. A sophisticated jet target could be the solution. A positive point is that the final state is sharp and the spectrum would be very narrow with a high-resolution detector. The other method could be a measurement of this  $\gamma$ -ray following the population of the  $2^+$  state in  $^{11}\text{B}(p, \alpha)$  reaction at a resonant proton energy of 163 keV. A comparison of the  $\gamma$ -yield and the  $\alpha$ -yield would extract the  $\gamma$ -branching ratio for this state and, hence, the required cross-section. However, very low coincidence count rates and the associated chance coincidence problem would be challenging. Finally, another interesting measurement that can be done in  $^8\text{Be}$  is on the intraresonance  $\gamma$ -transition in the broad  $4^+$  resonance. This should give information on the diagonal  $E2$  moment related to the quadrupole moment of the  $4^+$  state.

## Acknowledgement

This paper has been presented on behalf of the author's collaborators, V M Datar, Suresh Kumar, V Nanal, S P Behera, A Chatterjee, D Jenkins, C J Lister, E T Mirgule, A Mitra, S Pastore, R G Pillay, K Ramachandran, O J Roberts, P C Rout, A Shrivastava, P Sugathan

and R B Wiringa. The author acknowledges Late Prof C V K Baba, who was enthusiastic about this program, for very useful discussion. R Kujur and M Pose are thanked for their assistance during the experiment.

## References

- [1] K Ikeda, N Tagikawa and H Horiuchi, *Prog. Theor. Phys.* **464** (Suppl.) (1968)
- [2] F Hoyle, *Astrophys. J.* (Suppl. **1**) 121 (1954)
- [3] A Bohr and B R Mottelson, *Nuclear structure* (Benjamin, New York, 1975) Vol. II, p. 99–102 and references therein
- [4] R B Wiringa, S C Pieper, J Carlson and V R Pandharipande, *Phys. Rev. C* **62**, 014001 (2000)
- [5] U Peyer, J Hall, T Muller, M Suter and W Wofli, *Phys. Lett. B* **41**, 151 (1972)
- [6] B Frois, J Birchall, C R Lamontagne, U von Moellendorff, R Roy and R J Slobodrian, *Phys. Rev. C* **8**, 2132 (1973)
- [7] A M Green and J Niskanen, *Nucl. Phys.* **240**, 263 (1975)
- [8] D Baye and P Descouvemont, *Nucl. Phys. A* **443**, 302 (1985)
- [9] K Langanke, *Phys. Lett. B* **174**, 27 (1986)
- [10] S Ali and A R Bodmer, *Nucl. Phys.* **80**, 99 (1966)
- [11] B Buck, H Fredrich and C Wheatley, *Nucl. Phys. A* **275**, 246 (1977)
- [12] R B Wiringa, private communication
- [13] from Micron Semiconductor Ltd., United Kingdom
- [14] A Chatterjee, <http://www.tifr.res.in/~pell/lamps>
- [15] GEANT, version 3.21, CERN program library
- [16] V M Datar, Suresh Kumar, D R Chakrabarty, V Nanal, E T Mirgule, A Mitra and H H Oza, *Phys. Rev. Lett.* **94**, 122502 (2005)
- [17] J Dohet-Eraly and D Baye, *Phys. Rev. C* **88**, 024602 (2013)
- [18] K Langanke and C Rolfs, *Z. Phys. A* **324**, 307 (1986); *Phys. Rev. C* **33**, 790 (1986)
- [19] V M Datar *et al.*, *Phys. Rev. Lett.* **111**, 062502 (2013)
- [20] K M Nolle, S C Pieper, R B Wiringa, J Carlson and G M Hale, *Phys. Rev. Lett.* **99**, 022502 (2007)